

UCLA/93/TEP/36  
DTP/93/80  
hep-ph/9312218  
October 1993

# Supersymmetry Relations Between Contributions To One-Loop Gauge Boson Amplitudes

Z. Bern  
*Department of Physics*  
*UCLA*  
*Los Angeles, CA 90024*

and

A.G. Morgan  
*Department of Physics*  
*University of Durham*  
*Durham DH1 3LE, England*

## Abstract

We apply ideas motivated by string theory to improve the calculational efficiency of one-loop weak interaction processes with massive external gauge bosons. In certain cases “supersymmetry” relations between diagrams with a fermion loop and with a gauge boson loop hold. This is explicitly illustrated for a particular one-loop standard model process with four-external gauge bosons. The supersymmetry relations can be used to provide further significant improvements in calculational efficiency.

## 1. Introduction.

Even the simplest one-loop gauge boson amplitudes can be rather formidable to compute. Recently an advance in the calculation of one-loop gauge boson amplitudes has been made based on string theory [1,2]. Using this technique the first calculation of the one-loop five-gluon amplitude has been performed [3,4]. As another example, one-loop graviton scattering calculations become relatively simple once the corresponding QCD calculations have been performed [5].

In the case of QCD, the string-based rules have been interpreted in terms of a particular set of vertices and organizations whose main feature is that they lead to relatively efficient computations. As a bonus, the various contributions to the one-loop amplitude exhibit simple relations between the gluon and fermion contributions at the level of the integrands.

In the usual Feynman diagram approach the initial lorentz structure of the various diagrams bear little resemblance to each other. Each of the different types of Feynman diagrams are then separately evaluated. This may be contrasted to string theory, where the various particle states are treated more uniformly, making relationships between the various types of contributions apparent. In the calculation of the five-gluon amplitude [3], a striking manifestation of this is that the gluon loop contribution is rather easy to obtain from the fermion loop contribution since the two calculations are almost identical. These relations between fermion and boson loop contributions are connected to the remarkable simplicity of one-loop amplitudes in  $N = 4$  super-Yang-Mills, which was first pointed out with the aid of string theory [6]. Supersymmetry relations are by now a standard tool in QCD calculations [7]. The conventional supersymmetry relations are between amplitudes with differing numbers of external fermions. The relations we discuss here are between diagrams with the same type of external particles but with differing internal particles.

Here we explain how to reorganize one-loop gauge boson amplitudes involving  $W$ 's and  $Z$ 's to mimic the efficient reorganization for gluons. As an added bonus in certain cases the manifest relations between gauge boson and fermion loops are preserved. These relations can then be used to provide further significant reductions in the amount of work involved in a computation. To do this, we will make direct use of the field theory lessons obtained from string theory [8,9]. The approach presented here is helpful whenever a one-loop diagram contains a non-abelian vertex.

As a particular example, we will discuss the calculation of the process  $Z \rightarrow 3\gamma$

[10,11] (which is of some interest for compositeness searches). From the results of a unitary gauge calculation, in ref. [11] the striking relationship between the boson and fermion contributions to the amplitude was already noted. We will explicitly show how to make use of this supersymmetry relationship to significantly improve calculational efficiency for this process. With the superstring-motivated reorganization nearly the entire result for the  $W$ -loop contributions can be obtained from the fermion loop contribution. In processes such as  $2\gamma \rightarrow 2Z$  [12] (which is of some interest for searches for ultra-heavy fermions at future photon-photon colliders) there are additional mixed scalar and gauge-boson loops, but one can still use the supersymmetry relations to significantly reduce the computational difficulty of the gauge-boson loop contributions. For processes, with external  $W$ 's one loses simple supersymmetry relations due to the flavor changing in the loop, but there are still significant advantages to the gauge choices which we describe.

In section 2 we review the supersymmetry relations for the diagrams that appear in one-loop gauge boson scattering calculations and describe the application to spontaneously broken theories such as the standard model. In section 3 we present the calculation of  $Z \rightarrow 3\gamma$  as an explicit example. In section 4 we comment on other processes such as  $2\gamma \rightarrow 2Z$  and provide tables containing the coupling constants for the various vertices.

## 2. $N = 4$ supersymmetry relations.

Although derived from string theory, the string-based organization can be understood in ordinary field theory [8,2]. Besides the inherent advantage of obtaining simpler diagrams with an efficient organization, as an added bonus one obtains relations, connected to the simplicity of  $N = 4$  super-Yang-Mills amplitudes, between gauge-boson and fermion loop diagrams. The use of these  $N = 4$  supersymmetry relations as a computational tool was pointed out in ref. [3] for the one-loop five-gluon amplitude. With the string-based organization the relations are manifest at the level of the integrands of diagrams and can be effectively used as a computational tool to obtain most of the gauge boson loop contribution from the fermion loop contribution.

Following the discussion of refs. [8,2] the key field theory ingredients for obtaining a good fraction of the gluon amplitude simplifications of the string-based approach are:

- 1) The Feynman rules should be color ordered [13,2]. To a large extent this simply amounts to rewriting the Yang-Mills structure constants in terms of traces of

commutators of fundamental representation matrices and considering only one color structure at a time. This concept is useful in QCD because it reduces the number of diagrams to be considered.

- 2) Background field Feynman gauge [14] should be used in calculations where a non-abelian vertex appears in the loop. This gauge is used to construct the one particle irreducible diagrams describing a gauge invariant effective action. The background field Feynman gauge is advantageous to use because the vertices are simpler than in the conventional Feynman gauge. For the  $N = 4$  supersymmetry identities to be manifest it is essential for all vertices of the one-particle irreducible diagrams to be background field gauge vertices.
- 3) The second order formalism should be used for the vector part (no  $\gamma_5$ ) of one particle irreducible diagrams with fermion loops [8]. This formalism amounts to rewriting the usual Dirac determinant (for a fermion of unit coupling) as

$$\begin{aligned}\det[\not{D} + im] &= \{\det[(\not{D} - im)(\not{D} + im)]\}^{1/2} \\ &= \{\det[D^2 - \frac{1}{2}\sigma^{\mu\nu}F_{\mu\nu} + m^2]\}^{1/2}.\end{aligned}\tag{1}$$

With this formalism, the fermion loop contributions are very similar to those of the gauge bosons. Additionally, there is considerable overlap with the calculation of ghost or scalar loop contributions.

- 4) The scattering amplitudes are constructed by sewing trees onto the one-particle irreducible diagrams. One can use standard Feynman gauge for the trees if one desires. For gluons, a particularly convenient gauge for the trees is the non-linear Gervais-Neveu gauge [15,8] because of the simple vertices. It is obviously advantageous to use different gauges for the tree and loop parts of the computation since one can optimize the gauge choices to minimize the computations required in the different parts of the diagrams. (Although it might seem strange that two different gauge choices are used for the loop and tree parts of the Feynman diagrams, in the background field method this has been justified by Abbott, Grisaru and Schaeffer [14]).
- 5) With the background field Feynman gauge and second order fermion formalism for the one-particle irreducible diagrams, virtually the entire calculation of a gauge boson loop is contained in the fermion loop calculation. This can be used to avoid pointless duplication of significant portions of the calculation.

6) Finally, a decomposition into gauge invariant tensors [16,11] or spinor helicity methods [17] can be used. In this paper we use the former method. With the tensor decomposition method one can use the usual Passarino-Veltman [18] technique for performing tensor integrals. To use the spinor helicity technique one first performs those spinor simplifications which are not obstructed by the presence of loop momentum. Then a Feynman parametrization is performed to eliminate the loop momentum; the remaining spinor helicity simplifications can then be performed. (One can use an electric circuit analogy [19] to arrive at the same integrand if one desires.) The Feynman parameter integrals can then be evaluated using the integration method of ref. [4].

Here we apply the latter five ideas to weak interactions and demonstrate that the gain in computational efficiency is quite significant. The application of these ideas is straightforward since it mainly involves using a different set of Feynman rules than the conventional ones and then observing a set of relationships between the integrands of certain diagrams. In the string-based approach of refs. [1,8] these relations are an inherent property of the string-based rules. In the above field theory approach, the relations are found after the trace over  $\gamma$ -matrices has been performed and the integrands of the various loop contributions are compared. We now present the application of the above ideas to weak interactions.

First consider the case of no fermions. In the background field Feynman gauge [14] this sector of the  $SU(2) \times U(1)$  Lagrangian is given by  $\mathcal{L}_1 + \mathcal{L}_2 + \mathcal{L}_{gf} + \mathcal{L}_{ghost}$  where,

$$\begin{aligned}
\mathcal{L}_1 &= -\frac{1}{4}(F_i^{\mu\nu}(\tilde{W} + W))^2 - \frac{1}{4}(F^{\mu\nu}(\tilde{B} + B))^2 \\
\mathcal{L}_2 &= (D_\mu \phi)^\dagger (D^\mu \phi) - \lambda(\phi^\dagger \phi)^2 + \mu^2 \phi^\dagger \phi \\
\mathcal{L}_{gf} &= -\frac{1}{2}(\partial_\mu W^{i\mu} + g\epsilon^{ijk}\tilde{W}_{j\mu}W_k^\mu + \frac{ig}{2}(\phi'^\dagger T^i \phi_0 - \phi_0^\dagger T^i \phi'))^2 \\
&\quad - \frac{1}{2}(\partial_\mu B^\mu + \frac{ig'}{2}(\phi'^\dagger \phi_0 - \phi_0^\dagger \phi'))^2 \\
\mathcal{L}_{ghost} &= -\omega_i^\dagger \left( \partial^2 \delta^{il} - g\overleftarrow{\partial}_\mu \epsilon^{ijl}(W_j^\mu + \tilde{W}_j^\mu) + g\epsilon^{ijl}\tilde{W}_j^\mu \overrightarrow{\partial}_\mu + g^2 \tilde{W}_j^\mu (W_m^\mu + \tilde{W}_m^\mu) \epsilon^{ijk} \epsilon^{kml} \right. \\
&\quad \left. + \frac{g^2}{4}(\phi^\dagger T^l T^i \phi_0 + \phi_0^\dagger T^i T^l \phi) \right) \omega_l - b^\dagger \left( \partial^2 + \frac{g'^2}{4}(\phi^\dagger \phi_0 + \phi_0^\dagger \phi) \right) b \\
&\quad - \omega_i \frac{gg'}{4}(\phi^\dagger T^i \phi_0 + \phi_0^\dagger T^i \phi) b - b^\dagger \frac{gg'}{4}(\phi^\dagger T^l \phi_0 + \phi_0^\dagger T^l \phi) \omega_l
\end{aligned} \tag{2}$$

where  $T^i$  are the Pauli spin matrices and  $\tilde{W}^i$  and  $\tilde{B}$  are respectively the  $SU(2)$  and  $U(1)$  hypercharge background fields and  $W^i$  and  $B$  are the corresponding quantum fields. The covariant derivatives appearing in  $\mathcal{L}_2$  are covariant with respect to both quantum and background fields. The ghost Lagrangian may be obtained by the usual Faddeev-Popov technique. In order to obtain the usual fields of the standard model we shift the Higgs field  $\phi = \phi_0 + \phi'$  with

$$\phi_0 = \begin{pmatrix} 0 \\ v/\sqrt{2} \end{pmatrix} \quad \phi' = \begin{pmatrix} \phi^+ \\ (H + i\chi)/\sqrt{2} \end{pmatrix} \quad (3)$$

with  $v = (\mu^2/\lambda)^{\frac{1}{2}}$  and define

$$\begin{aligned} \tilde{W}_\mu^1 &= (\tilde{W}^+ + \tilde{W}^-) / \sqrt{2} \\ \tilde{W}_\mu^2 &= (\tilde{W}^+ - \tilde{W}^-) i / \sqrt{2} \\ \tilde{W}_\mu^3 &= \cos \theta_W \tilde{Z}_\mu + \sin \theta_W \tilde{A}_\mu \\ \tilde{B}_\mu &= -\sin \theta_W \tilde{Z}_\mu + \cos \theta_W \tilde{A}_\mu \end{aligned} \quad (4)$$

with similar equations for the quantum and ghost fields.

After performing the shifts of field variables in eqs. (2) and (3) we obtain the gauge sector of the standard model Lagrangian in background field Feynman gauge. The Feynman rules generated by this Lagrangian relevant for the calculation of  $Z \rightarrow 3\gamma$  are depicted in fig. 1. Only those vertices with two quantum fields attached are given since those are the only contributing ones at one loop. These Feynman rules satisfy the property that there is no  $\tilde{A}\phi W^\pm$  coupling, considerably reducing the number of diagrams which must be considered in the  $Z \rightarrow 3\gamma$  calculation, since diagrams with mixed  $\phi$ - $W$  loops do not appear. (This is similar to the absence of such couplings in the non-linear  $R_\xi$  gauges discussed in refs. [20].) For generality the coupling constants in the rules of fig. 1 have been removed since the various types of gauge bosons couple with different strengths. The various coupling constants required for the calculation of  $Z \rightarrow 3\gamma$  are given in Table 1.

Vertex	Coefficient
$\tilde{A}W^-W^+$	$e$
$\tilde{Z}W^-W^+$	$e/\tan\theta_W$
$\tilde{A}\phi^-\phi^+, \tilde{A}\omega^{+\dagger}\omega^+, \tilde{A}\omega^-\omega^{-\dagger}$	$-e$
$\tilde{Z}\phi^-\phi^+$	$-e/\tan 2\theta_W$
$\tilde{Z}\omega^{+\dagger}\omega^+, \tilde{Z}\omega^-\omega^{-\dagger}$	$-e/\tan\theta_W$
$\tilde{A}\tilde{A}\phi^+\phi^-, \tilde{A}\tilde{A}\omega^{\pm\dagger}\omega^\pm$	$e^2$
$\tilde{A}\tilde{Z}\phi^+\phi^-$	$e^2/\tan 2\theta_W$
$\tilde{A}\tilde{Z}\omega^{\pm\dagger}\omega^\pm$	$e^2/\tan\theta_W$
$\tilde{A}\tilde{A}W^-W^+,$	$e^2$
$\tilde{A}\tilde{Z}W^-W^+,$	$e^2/\tan\theta_W$

**Table 1:** The coupling constants of the vertices needed for the calculation of  $Z \rightarrow 3\gamma$ .

Now consider the inclusion of internal fermions with no flavor changing in the loop. Because the relationship between the fermion and boson loop that we are interested in does not involve the  $\gamma_5$  in the fermion coupling we divide the fermion loop computation into a part which contains a  $\gamma_5$  and a part which does not contain a  $\gamma_5$ . This can be done by considering the one-particle irreducible diagrams in the conventional (first order) formalism; one then collects all the  $\gamma_5$ 's together so that the fermion trace contains a single  $\gamma_5$ . This is then split into the axial part containing the  $\gamma_5$  and the vector part which does not contain the  $\gamma_5$ . The axial part may be evaluated in the usual way since this part does not play a role in the supersymmetry identities. The diagrams of the vector part of the one-loop effective action may be described by the familiar Dirac determinant which is rewritten in the second order form (1). It is this form which makes the relationship of the fermion loop to the gauge boson loop manifest in the integrands. For the case where there is flavor changing within the loop, and necessarily different masses appear inside it, the relationship to the gauge boson loop is more obscure and one loses the added bonus of simple supersymmetry relations; the advantage of simpler background field vertices is, of course, not lost.

In particular, for the case of  $Z \rightarrow 3\gamma$  the  $\gamma_5$  contributions all drop out because of cancellations between diagrams where the fermion circulates in one direction and diagrams where the fermion circulates in the opposite direction. This means that for this process the entire fermion loop can be rewritten in the second order form [8,2]

$$\Gamma_{\text{fermion}}[\tilde{W}^i, \tilde{B}] = \frac{1}{2} \ln \det [D^2(\tilde{W}^i, \tilde{B}) - \frac{1}{2}\sigma^{\mu\nu}\mathbf{F}_{\mu\nu}(\tilde{W}^i) - \frac{1}{2}\sigma^{\mu\nu}F_{\mu\nu}(\tilde{B}) + m^2] \quad (5)$$

where the replacement in eq. (4) should be carried out to obtain the usual fields of the standard model. By expanding out this determinant we obtain the one-loop Feynman rules for internal fermions depicted in fig. 2. The coupling associated with each background field is the same as the appropriate effective vector coupling of the first order formalism with an accompanying loop factor  $-1/2$ , where the minus sign is the familiar one for a fermion loop. One obvious feature of these second order fermion rules is that they bear a much greater resemblance to the boson rules than the conventional (first order formalism) Feynman rules for fermions; this is important for making the supersymmetry relations hold diagram-by-diagram.

With the rules given in figs. 1 and 2 the *integrands* of diagrams for one-loop  $n$  gauge boson scattering satisfy an  $N = 4$  supersymmetry constraint [3,2]. This relationship between diagrams with fermions in the loop and gauge bosons (and associated ghosts) in the loop is depicted in fig. 3 and is given by

$$\begin{aligned} D^{\text{scalar}}(m_s) &= C_s S(m_s) \\ D^{\text{fermion}}(m_f) &= -C_f (2S(m_f) + F(m_f)) \\ D^{\text{gauge boson}}(m_g) &= C_g ((1 - \delta_R \epsilon) 2S(m_g) + 4F(m_g) + G(m_g)) \end{aligned} \tag{6}$$

where the particle labels refer to the states circulating in the loop, the  $m_x$  are the masses of the particles circulating in the loop and the  $C_i$  are coupling constant factors which depend on the processes under consideration. The  $D$  all refer to the same diagram types, but with different particles circulating in the loops. For two or three legs attached to the loop the simple quantity  $G$  vanishes at the level of the integrand. (The dimensional regularization parameter is  $\delta_R = 1$  for either conventional dimensional regularization or for the 't Hooft-Veltman scheme [21] while  $\delta_R = 0$  for either the dimensional reduction [22] or four-dimensional helicity [1] schemes.) In cases where all types of diagrams satisfy the supersymmetry identities (6) (such as  $Z \rightarrow 3\gamma$ ), the sum over all diagrams – namely the amplitude – also satisfies this identity.

The connection of these identities to  $N = 4$  supersymmetry is that for  $N = 4$  super-Yang-Mills (one gluon, four Weyl fermions, and 6 real scalars) everything but  $G$  cancels after summing over the various loop contributions. (The regulator factor  $\delta_R = 0$  is necessary so that supersymmetry is not broken). That is,

$$D^{N=4 \text{ susy}} = g^4 G \tag{7}$$

where  $g$  is the coupling. The other terms all cancel.



In performing the calculation, instead of calculating the diagrams directly it is more efficient to calculate  $S$ ,  $F$  and  $G$ . The importance of the above identities is that each part of the calculation is successively easier to perform;  $S$  is the most complicated part,  $F$  is the next most complicated part and  $G$  is by far the easiest part of the calculation. In a conventional approach one would effectively be recomputing the  $S$  and  $F$  parts since one computes the gauge boson loop directly. This leads to a significant computational advantage for the gauge boson loop beyond the already large simplifications of Feynman background field gauge. (With conventional gauge choices, like 't Hooft-Feynman or unitary gauge, the unnecessary recomputation of  $S$  and  $F$  is actually significantly more complicated than the direct computation of these quantities from scalar and fermion loops.)

### 3. Explicit example.

Consider the process  $Z \rightarrow 3\gamma$ . This process has already been discussed in refs. [10,11] using more conventional techniques. We show here how to reduce the  $W$ -loop computation to a very simple one once the fermion loop is calculated. The four one-loop diagram types required for calculating  $Z \rightarrow 3\gamma$  are depicted in fig. 4. The complete amplitude is obtained by summing over the six permutations of external legs.

From ref. [11] we have the general tensor consistent with gauge invariance and crossing symmetry for the three photons as

$$\begin{aligned} \mathcal{M}^{\alpha\mu\nu\rho}(p_1, p_2, p_3) = & A_1(p_1, p_2, p_3) \frac{1}{p_1 \cdot p_3} \left( \frac{p_3^\mu p_1^\rho}{p_1 \cdot p_3} - g^{\mu\rho} \right) p_1^\alpha \left( \frac{p_3^\nu}{p_2 \cdot p_3} - \frac{p_1^\nu}{p_1 \cdot p_2} \right) \\ & + A_2(p_1, p_2, p_3) \left\{ \frac{1}{p_2 \cdot p_3} \left( \frac{p_1^\alpha p_3^\mu}{p_1 \cdot p_3} - g^{\alpha\mu} \right) \left( \frac{p_1^\nu p_2^\rho}{p_1 \cdot p_2} - g^{\nu\rho} \right) \right. \\ & \quad \left. + \frac{1}{p_1 \cdot p_3} \left( \frac{p_1^\nu}{p_1 \cdot p_2} - \frac{p_3^\nu}{p_2 \cdot p_3} \right) (p_1^\rho g^{\alpha\mu} - p_1^\alpha g^{\mu\rho}) \right\} \\ & + A_3(p_1, p_2, p_3) \frac{1}{p_1 \cdot p_3} \left( \frac{p_1^\alpha p_3^\mu}{p_1 \cdot p_3} - g^{\alpha\mu} \right) \left( \frac{p_3^\nu p_2^\rho}{p_2 \cdot p_3} - g^{\nu\rho} \right). \end{aligned} \tag{8}$$

The amplitude is obtained from this tensor by dotting it into the external polarization vectors. In this method one only computes the scalar quantities  $A_1$ ,  $A_2$ ,  $A_3$  thereby eliminating the redundant information contained in a gauge invariant expression, in a way analogous to what happens with spinor helicity methods. Factoring out the coupling constants we obtain an expression for the  $A_i$ 's in terms of the scalar, fermionic

and gauge boson Feynman rules of figs. 1 and 2 (c.f. (12) of [11])

$$A_i(p_1, p_2, p_3) = \frac{ie^4}{8\pi^2 \sin 2\theta} \left( \sum_f e_f^3 v_f A_i^f(s, t, m_f) + \cos^2 \theta_W A_i^W(s, t, M_W) + \frac{\cos 2\theta_W}{2} A_i^\phi(s, t, M_W) \right) \quad (9)$$

where the fermionic  $A_i$ 's are defined to include their overall minus sign. For the gauge loop we note that the inclusion of both ghosts,  $\omega^\pm$  and  $\omega^{\pm\dagger}$  is straightforward since they are just (fermionic) complex scalar fields. In fact, in background field gauge,  $A_i^{\omega^\pm}(s, t, M_W) = -A_i^\phi(s, t, M_W)$ , and thus  $A_i^W$ , which we take to include both the  $W$  and Faddeev-Popov ghost contributions, is obtained by application of the Feynman rules of fig. 1 minus twice the scalar  $A_i^\phi$  result. We therefore only need to compute the three separate contributions  $A_i^\phi$ ,  $A_i^f$  and  $A_i^W$ . Further discussion of the tensor decomposition method can be found in refs. [16,11].

In order to minimize the duplication of effort we make use of the supersymmetry relations (6) to systematize our evaluation of the above scalar  $A_i$  functions. Since all of the diagram types in this calculation satisfy the supersymmetry relation (6) the sum over the diagrams or amplitude will satisfy the relation. As mentioned previously, it is not difficult to verify that the  $\gamma_5$  contribution in the fermion loop drops out because of cancellations between diagrams where the fermion circulates in one direction and diagrams where the fermion circulates in the opposite direction. This means that the entire fermion loop contribution is of the vector type and therefore included in the supersymmetry identity.

The first step is to compute the scalar loop contribution. After summing over diagrams and reducing the tensor integral down to scalar ones [18] the result is

$$\begin{aligned} A_1^\phi(s, t, m) &= \mathcal{S}_1(s, t, m) = -\frac{1}{2} A_1^f(s, t, m), \\ A_2^\phi(s, t, m) &= \mathcal{S}_2(s, t, m) = -\frac{1}{2} A_2^f(s, t, m) - \frac{tu}{2} \left( 2m^2 H(m) - \frac{1}{s} E(t, u, m) \right), \\ A_3^\phi(s, t, m) &= \mathcal{S}_3(s, t, m) = -\frac{1}{2} A_3^f(s, t, m) - \frac{1}{2t} \left\{ t^2 E(s, t, m) - u^2 E(u, s, m) \right. \\ &\quad \left. + 2m^2 ut(u - t) H(m) \right\} \end{aligned} \quad (10)$$

where the  $A_i^f$  are functions defined in ref. [11] and

$$\begin{aligned}
E(s, t, m) &= s C(s, m) + s_1 C_1(s, m) + t C(t, m) + t_1 C_1(t, m) - st D(s, t, m), \\
H(m) &= D(s, t, m) + D(t, u, m) + D(u, s, m) \\
s_1 C_1(s, m) &= s C(s, m) - M_Z^2 C(M_Z^2, m)
\end{aligned} \tag{11}$$

The mass  $m$  is the mass of the scalar going around the loop and  $s = (p_1 + p_2)^2$ ,  $t = (p_1 + p_4)^2$  and  $u = (p_1 + p_3)^2$  are Mandelstam variables, and  $s_1 = s - M_Z^2$ ,  $t_1 = t - M_Z^2$  and  $u_1 = u - M_Z^2$ . For convenience we quote the simplest of these functions here as

$$\begin{aligned}
\mathcal{S}_1(s, t, m) &= -\frac{2st}{t_1} - \frac{4t}{u} \left( s B_1(s, m) - s_1 B_1(t, m) \right) + \frac{2M_Z^2(s+2u)t}{t_1^2} B_1(t, m) \\
&\quad - \frac{st(2t+u)}{u^2} E(s, t, m) - \frac{4m^2 t}{u} E(s, t, m) - \frac{2m^2 t}{s} E(t, u, m) \\
&\quad - 2m^2 \left( s C(s, m) + t C(t, m) + u_1 C_1(u, m) \right) \\
&\quad + \frac{4m^2(s+2u)t}{t_1} C_1(t, m) + \frac{2m^2 st(u+2t)}{u} D(s, t, m) \\
&\quad + m^2 \left( ut D(t, u, m) + st D(s, t, m) + us D(u, s, m) \right) + 4m^4 t H(m)
\end{aligned} \tag{12}$$

with  $B_1(s, m) = B(s, m) - B(M_Z^2, m)$ . The scalar loop is the most complicated piece to integrate since the graphs contain the most powers of loop momentum in the numerator. In general, because of the explosion of terms which occurs in the evaluation of tensor integrals [18,4], factors of loop momenta cause the largest complications; this is reflected in the complexity of this result.

The next stage of the computation is to subtract out the part of the fermion loop proportional to the scalar loop in the integrand of each diagram; after integration this yields the  $\mathcal{F}_i$  which after summing over diagrams are as follows

$$\begin{aligned}
\mathcal{F}_1(s, t, m) &= -A_1^f(s, t, m) - 2\mathcal{S}_1(s, t, m) = 0, \\
\mathcal{F}_2(s, t, m) &= -A_2^f(s, t, m) - 2\mathcal{S}_2(s, t, m) = tu \left( 2m^2 H(m) - \frac{1}{s} E(t, u, m) \right), \\
\mathcal{F}_3(s, t, m) &= -A_3^f(s, t, m) - 2\mathcal{S}_3(s, t, m) = \frac{1}{t} \left\{ t^2 E(s, t, m) - u^2 E(u, s, m) \right. \\
&\quad \left. + 2m^2 ut(u-t) H(m) \right\}.
\end{aligned} \tag{13}$$

The required integrals are much simpler quantities than for  $\mathcal{S}_i$  since the integrands contain at most two powers of loop momentum instead of four. The relative simplicity of the computation as compared to the scalar loop calculation is reflected in the relative simplicity of the results. Plugging the  $\mathcal{S}_i$  and  $\mathcal{F}_i$  into the second of the supersymmetry relations in eq. (6) reproduces the results for fermion loops of ref. [11].

To obtain the  $W^\pm$  loop contribution in each diagram we subtract the integrands associated with  $2\mathcal{S}(s, t, M_W) + 4\mathcal{F}(s, t, M_W)$  from the full expression for the  $W^\pm$  loop (including Fadeev-Popov ghosts); this leaves only box diagrams to be evaluated since all other integrands cancel by the supersymmetry relations given in fig. 3. Furthermore, the only terms in the vertices which contribute are those which contain no loop momentum, the ones containing loop momentum manifestly cancel in the calculation of  $\mathcal{G}(s, t, M_W)$ . This cancellation is a direct consequence of the  $N = 4$  supersymmetry relations. Since the terms with loop momentum cancel,  $\mathcal{G}$  is reduced to a relatively simple algebraic expression times a scalar box integral, which may be obtained from ref. [23]. Since there is no need to evaluate a tensor integral, this part of the computation is relatively trivial. (Indeed, by using rules of the string based type [1,2] it is possible to write down the answer without calculation.) For the diagrams with a 1,2,3,4 and reversed ordering of legs the remaining kinematic tensor is simple and given by

$$\begin{aligned}
G^{\alpha\mu\nu\rho}(1234) = & -D(s, t) \left( 8 \left( g^{\alpha\mu} g^{\nu\rho} su + g^{\alpha\nu} g^{\mu\rho} st + g^{\alpha\rho} g^{\mu\nu} ut \right) \right. \\
& + 16s \left( g^{\alpha\rho} p_3^\mu p_3^\nu + p_3^\mu (g^{\nu\rho} p_2^\alpha - g^{\alpha\nu} p_2^\rho) + p_3^\nu (g^{\mu\rho} p_1^\alpha - g^{\alpha\mu} p_1^\rho) \right) \\
& + 16t \left( g^{\alpha\mu} p_1^\nu p_1^\rho + p_1^\nu (g^{\mu\rho} p_3^\alpha - g^{\alpha\rho} p_3^\mu) + p_1^\rho (g^{\mu\nu} p_2^\alpha - g^{\alpha\nu} p_2^\mu) \right) \\
& \left. + 16u \left( g^{\alpha\nu} p_2^\mu p_2^\rho + p_2^\rho (g^{\mu\nu} p_1^\alpha - g^{\alpha\mu} p_1^\nu) + p_2^\mu (g^{\nu\rho} p_3^\alpha - g^{\alpha\rho} p_3^\nu) \right) \right)
\end{aligned} \tag{14}$$

where we have organized the terms to exhibit manifest gauge invariance. The other orderings of external legs are obtained by a relabeling of legs. After summing over the independent orderings and comparing to the kinematic tensor (8) and using

$$\mathcal{G}_i(s, t, M_W) = A_i^W(s, t, M_W) - (2\mathcal{S}_i(s, t, M_W) + 4\mathcal{F}_i(s, t, M_W)) \tag{15}$$

the result can be summarized in terms of the three scalar functions

$$\begin{aligned}
\mathcal{G}_1(s, t, M_W) &= 0, \\
\mathcal{G}_2(s, t, M_W) &= -2stuH(M_W), \\
\mathcal{G}_3(s, t, M_W) &= 0.
\end{aligned} \tag{16}$$

Again the simplicity of the calculation is reflected in the simplicity of the result. Inserting these functions into the supersymmetry identities (6) reproduces the results of ref. [11] for the gauge boson loop. In particular eliminating for  $\mathcal{S}_i$  in favor of  $A_i^f$ , and using the identity  $\cos 2\theta_W = \cos^2 \theta_W (2 - M_Z^2/M_W^2)$  we find that the non-fermionic contribution to the  $Z\gamma\gamma\gamma$  scattering tensor

$$\begin{aligned} A_i^b &= A_i^W + \frac{\cos 2\theta_W}{2} A_i^\phi \\ &= \frac{1}{4} \left( \frac{M_Z^2}{M_W^2} - 6 \right) A_i^f + \frac{1}{4} \left( \frac{M_Z^2}{M_W^2} + 10 \right) \mathcal{F}_i + \mathcal{G}_i. \end{aligned} \quad (17)$$

This then provides an explanation for the empirically observed relations (15) of ref. [11]; namely that they are supersymmetry identities.

As a simple check on the results for  $\mathcal{G}$ , we have verified that for external mass  $M_Z \rightarrow 0$  the kinematic coefficient of the box diagram given in eq. (14) is proportional to the color ordered Yang-Mills tree. This is in agreement with expectations from superstring theory with  $N = 4$  space-time supersymmetry [6] where the one-loop four-point amplitude is also proportional to the tree.

The calculation we have presented for the  $W$  loop may be compared to the unitary gauge calculation presented in ref. [11]. In that paper, the unitary gauge was used because of the significant reduction in the number of diagrams as compared to the standard 't Hooft-Feynman gauge. In the string-motivated organization presented here we have retained all the diagrammatic advantages of the unitary gauge. In addition, since it has been possible to use a simple Feynman type background field gauge it has not been necessary at any stage to cancel superficial ultra-violet divergences arising from the extra powers of momentum in the unitary gauge propagator. (This was the most time consuming part of the tensor reduction of ref. [11]). Furthermore, the vertices of background field 't Hooft-Feynman gauge are simpler than those of the unitary gauge. Finally, by making use of the  $N = 4$  supersymmetry relations we have reduced the  $W$ -loop calculation to that of simple scalar box integrals which are given in refs. [23]. The reorganization we have presented therefore represents a clear computational advantage.

What about the fermion loop part of the calculation? Superficially it might seem that since there are *four* diagram types in the second order formalism (figs. 2 and 4), instead of a single diagram type in the more usual spinor based (first order) formalism this represents a retrograde step in the calculational technique. In fact, the use of the second order formalism significantly improves the calculational efficiency of the fermion

loops since most of the calculation can be directly obtained from the calculation of scalars or ghosts in the loop. The similarity in structure of the fermion to scalar vertices (figs. 1 and 2) ensures that when calculating the  $\mathcal{F}_i$  the cancellations between the scalar and fermion loops implied by the supersymmetry equations (6) occur *on the first line* at the level of the integrand and before the evaluation of any tensor integrals. (Even if one were not interested in scalar or gauge boson loop contributions, it is generally still advantageous to break the fermion loop contribution into two separate pieces since it is usually easier to handle smaller physical pieces in a large calculation.) The second order formalism therefore also represents a considerable advance in calculational efficiency for the vector part of fermion loops (with no flavor changing).

#### 4. Other Processes.

The string-motivated reorganization discussed above is useful for other amplitudes. For completeness the coupling constants for the various other vertices with external gauge bosons are presented in Tables 2-4. Besides the vertex structures already encountered in 1 there is an additional non-abelian vertex given in fig. 5; the coupling constants associated with this vertex are presented in Table 4.

Vertex	Coefficient
$\tilde{W}^+ A W^-, \tilde{W}^- W^+ A$	$e$
$\tilde{W}^+ Z W^-, \tilde{W}^- W^+ Z$	$e / \tan \theta_W$
$\tilde{Z} W^\pm \phi^\mp$	$-e^2 v / \sin \theta_W \sin 2\theta_W$
$\tilde{Z} Z H$	$2e^2 v / \sin^2 2\theta_W$
$\tilde{W}^\pm W^\mp H$	$e^2 v / 2 \sin^2 \theta_W$
$\tilde{W}^\pm W^\mp \chi$	$\mp i e^2 v / 2 \sin^2 \theta_W$
$\tilde{W}^\pm A \phi^\mp,$	$e^2 v / \sin \theta_W$
$\tilde{W}^\pm Z \phi^\mp,$	$e^2 v / \tan 2\theta_W \sin \theta_W$
$\tilde{W}^+ H \phi^-, \tilde{W}^- \phi^+ H$	$e / 2 \sin \theta_W$
$\tilde{W}^\pm \chi \phi^\mp$	$i e / 2 \sin \theta_W$
$\tilde{Z} \chi H$	$-i e / \sin 2\theta_W$

**Table 2:** The coupling constants associated with other three point vertices. Those involving an odd number of gauge fields may be found in fig. 1 and the remaining vertices involving two gauge fields are to be found in fig. 5.

Vertex	Coefficient
$\tilde{W}^+ \tilde{W}^- AA$	$e^2$
$\tilde{W}^+ \tilde{W}^- AZ$	$e^2 / \tan \theta_W$
$\tilde{Z} \tilde{Z} W^- W^+, \tilde{W}^+ \tilde{W}^- ZZ$	$e^2 / \tan^2 \theta_W$
$\tilde{W}^\pm \tilde{W}^\pm W^\mp W^\mp,$	$-e^2 / \sin^2 \theta_W$
$\tilde{W}^+ \tilde{W}^- \omega^{A\dagger} \omega^A$	$e^2$
$\tilde{W}^\pm \tilde{A} \omega^{\pm\dagger} \omega^A, \tilde{W}^\pm \tilde{A} \omega^{A\dagger} \omega^\mp$	$-e^2$
$\tilde{W}^+ \tilde{W}^- \omega^{\pm\dagger} \omega^\pm,$	$e^2 / \sin^2 \theta_W$
$\tilde{W}^\pm \tilde{W}^\pm \omega^{\pm\dagger} \omega^\mp,$	$-e^2 / \sin^2 \theta_W$
$\tilde{W}^\pm \tilde{Z} \omega^{\pm\dagger} \omega^A, \tilde{W}^\pm \tilde{Z} \omega^{A\dagger} \omega^\mp$ $\tilde{W}^\pm \tilde{A} \omega^{\pm\dagger} \omega^Z, \tilde{W}^\pm \tilde{A} \omega^{Z\dagger} \omega^\mp$	$-e^2 / \tan \theta_W$
$\tilde{Z} \tilde{Z} HH, \tilde{Z} \tilde{Z} \chi\chi$	$e^2 / \sin^2 2\theta_W$
$\tilde{Z} \tilde{Z} \phi^+ \phi^-$	$e^2 / \tan^2 2\theta_W$
$\tilde{W}^+ \tilde{W}^- \phi^+ \phi^-, \tilde{W}^+ \tilde{W}^- HH, \tilde{W}^+ \tilde{W}^- \chi\chi$	$e^2 / 4 \sin^2 \theta_W$
$\tilde{W}^\pm \tilde{A} H \phi^\mp$	$e^2 / 4 \sin \theta_W$
$\tilde{W}^\pm \tilde{Z} H \phi^\mp$	$-e^2 / 4 \cos \theta_W$
$\tilde{W}^\pm \tilde{A} \chi \phi^\mp$	$\pm i e^2 / 4 \sin \theta_W$
$\tilde{W}^\pm \tilde{Z} \chi \phi^\mp$	$\mp i e^2 / 4 \cos \theta_W$
$\tilde{W}^+ \tilde{W}^- \omega^{Z\dagger} \omega^A, \tilde{W}^+ \tilde{W}^- \omega^{A\dagger} \omega^Z$	$e^2 / \tan \theta_W$
$\tilde{W}^+ \tilde{W}^- \omega^{Z\dagger} \omega^Z, \tilde{Z} \tilde{Z} \omega^{\pm\dagger} \omega^\pm$	$e^2 / \tan^2 \theta_W$
$\tilde{W}^\pm \tilde{Z} \omega^{\pm\dagger} \omega^Z, \tilde{W}^\pm \tilde{Z} \omega^{Z\dagger} \omega^\mp,$	$-e^2 / \tan^2 \theta_W$

**Table 3:** The coupling constants associated with the various four-point vertices found in fig. 1.

Vertex	Coefficient
$\tilde{W}^\pm \tilde{A} W^\mp A$	$e^2$
$\tilde{W}^\pm \tilde{Z} W^\mp A, \tilde{W}^\pm \tilde{A} W^\mp Z$	$e^2 / \tan \theta_W$
$\tilde{W}^\pm \tilde{Z} W^\mp Z$	$e^2 / \tan^2 \theta_W$
$\tilde{W}^+ \tilde{W}^- W^+ W^-$	$-e^2 / \sin^2 \theta_W$

**Table 4:** The coupling constants associated with four-point vertices of the type in fig. 5

Using these tables, one could for example consider the one-loop process  $2\gamma \rightarrow 2Z$  [12] (which is of some interest to future photon-photon colliders). In this process one can again use the  $N = 4$  supersymmetry relations of fig. 3 to relate the diagrams with the  $W$  going around the loop to the diagrams with fermions going around the loop. In this

case, however, there are mixed diagrams with both  $W$ 's and  $\phi$ 's in the loop. Although such diagrams are apparently not simply related to fermion loop diagrams they are simpler to evaluate since they have a maximum of two powers of loop momentum in the numerator.

Due to the simplicity of the background field vertices as well as the supersymmetry relations (6), one can expect a significant efficiency over previous calculations of  $2\gamma \rightarrow 2Z$  [12]. For example in the one performed by Berger in standard 't Hooft-Feynman gauge, there were 188 diagrams to evaluate for the boson loop contributions. Since each of the vertices is relatively complicated compared to background field vertices, this calculation is significantly more complicated than one which follows the above strategy. Indeed, Bajc in his paper states that there are 608 terms in the  $W$  box diagram alone. We may also contrast the above strategy to the non-linear gauge used by Jikia in his calculation; we retain the advantage of eliminating the  $\tilde{A}\phi^\pm W^\mp$  vertex and have the additional advantages of having simpler vertices and supersymmetry relations between diagrams. A third alternative is the non-linear gauge used by Dicus and Kao which has the advantage of eliminating all remaining diagrams with mixed  $W$ - $\phi$  loops, but then the vertices are more complicated and one loses the supersymmetry relations for the unmixed diagrams. Due to the supersymmetry relations, the main part of each of these calculations only reproduces pieces already computed for the fermion loops.

The ideas discussed above can also be applied to the case of external fermions. In particular, background field Feynman gauge is still advantageous to use even when some external legs are fermions. As for the purely external gauge boson case it is also useful to identify parts of the calculation which are duplicated in the various diagrams. This type of strategy has already been successfully applied in the calculation of the one-loop corrections to four- [24] and five-parton [25] processes.

## 5. Conclusions.

Various contributions to gauge boson amplitudes have relations between them connected to the fact that amplitudes in  $N = 4$  super-Yang-Mills have extremely simple forms. These relations were first applied in the string-based calculation of gluon amplitudes [3,2]. In order to make practical use of the supersymmetry relations one needs a formalism where the relations hold between the integrands of diagrams. The guidance for constructing such a formalism is provided by string theory and amounts to special gauge choices and organizations of the diagrams.



In this paper we have described the supersymmetry relations in weak interaction processes which involve gauge bosons. These types of relationships were observed to hold in the explicitly computed weak interaction process  $Z \rightarrow 3\gamma$  [11], although in the unitary gauge where the calculation was performed the relations seem mysterious. We have shown how to reorganize this calculation as well as other processes so that the supersymmetry relations are manifest in all stages of the calculation. Important ingredients for making the relationships manifest in the diagrams are the background field Feynman gauge for the gauge-boson loops and the second order formalism for fermion loops. In this way the gauge boson and fermion loop computations have considerable overlap. The parts of the calculation which overlap do not need to be recomputed for the gauge boson loop contributions.

A practical consequence of the reorganized calculation and the manifest supersymmetry relations is that instead of the  $W$ -loop contribution being the most complicated part of the calculation it is relatively easy to obtain it using results from the fermion loop contribution.

We thank L. Dixon, D.C. Dunbar, E.W.N. Glover, D.A. Kosower, and D. Morris for helpful discussions and G. Chalmers for collaboration on early stages of this work. The work of ZB was supported in part by the US Department of Energy Grant DE-FG03-91ER40662 and in part by the Alfred P. Sloan Foundation Grant BR-3222. AGM would like to thank the United Kingdom Science and Engineering Research Council for the award of a Research Studentship, and further to acknowledge the kind hospitality of the UCLA Physics Department where this work was completed.

## References

- [1] Z. Bern and D.A. Kosower, Phys. Rev. Lett. 66:1669 (1991);  
 Z. Bern and D.A. Kosower, Nucl. Phys. B379:451 (1992);  
 Z. Bern and D.A. Kosower, in *Proceedings of the PASCOS-91 Symposium*, eds. P. Nath and S. Reucroft;  
 Z. Bern, Phys. Lett. 296B:85 (1992);  
 Z. Bern, L. Dixon and D.A. Kosower, unpublished.
- [2] Z. Bern, UCLA/93/TEP/5, hep-ph/9304249, proceedings of TASI 1992.
- [3] Z. Bern, L. Dixon and D.A. Kosower, Phys. Rev. Lett. 70:2677 (1993); in preparation.
- [4] Z. Bern, L. Dixon and D.A. Kosower, Phys. Lett. B302:299 (1993); SLAC-PUB-5947, to appear in Nucl. Phys. B.
- [5] Z. Bern, D.C. Dunbar, and T. Shimada, Phys. Lett. B312:277 (1993).
- [6] M.B. Green, J.H. Schwarz and L. Brink, Nucl. Phys. B198:472 (1982).
- [7] M.T. Grisaru, H.N. Pendleton and P. van Nieuwenhuizen, Phys. Rev. D15:996 (1977);  
 M.T. Grisaru and H.N. Pendleton, Nucl. Phys. B124:81 (1977);  
 S.J. Parke and T. Taylor, Phys. Lett. B157:81 (1985);  
 Z. Kunszt, Nucl. Phys. B271:333 (1986);  
 M.L. Mangano and S.J. Parke, Phys. Rep. 200:301 (1991).
- [8] Z. Bern and D.C. Dunbar, Nucl. Phys. B379:562 (1992).
- [9] M.J. Strassler, Nucl. Phys. B385:145 (1992);  
 M.G. Schmidt and C. Schubert, preprint HD-THEP-93-24, hep-th/9309055.
- [10] M. Baillargeon and F. Boudjema, Phys. Lett. B272:158 (1991);  
 X.Y. Pham, Phys. Lett. B272:373 (1991);  
 F.-X. Dong, X.-D. Jiang and X.-J. Zhou, Phys. Rev. D46:5074 (1992).
- [11] E.W.N. Glover and A.G. Morgan, Z. Phys. C60:175 (1993).
- [12] M. Chanowitz, Phys. Rev. Lett. 69:2037 (1992);  
 G.V. Jikia, Phys. Lett. B298:224 (1993); Nucl. Phys. B405:24 (1993);  
 B. Bajc, Phys. Rev. D48:1907 (1993);  
 M.S. Berger, preprint MAD/PH/771;  
 D. A. Dicus and C. Kao, FSU-HEP-930808, hep-ph/9308330;  
 A. Abbasabadi, D. Bowser-Chao, D.A. Dicus and W.W. Repko, MSUTH-92-03,

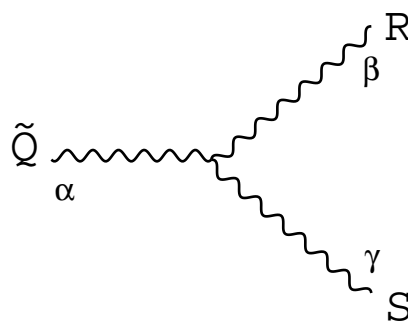
hep-ph/9301226.

- [13] J.E. Paton and H.M. Chan, Nucl. Phys. B10:516 (1969);  
F.A. Berends and W.T. Giele, Nucl. Phys. B294:700 (1987);  
M. Mangano and S.J. Parke, Nucl. Phys. B299:673 (1988);  
M. Mangano, Nucl. Phys. B309:461 (1988);  
Z. Bern and D.A. Kosower, Nucl. Phys. B362:389 (1991).
- [14] G. 't Hooft, Acta Universitatis Wratislavis no. 38, 12th Winter School of Theoretical Physics in Karpacz; *Functional and Probabilistic Methods in Quantum Field Theory*, Vol. 1 (1975);  
B.S. DeWitt, in *Quantum Gravity II*, eds. C. Isham, R. Penrose and D. Sciama (Oxford, 1981);  
L.F. Abbott, Nucl. Phys. B185:189 (1981);  
L.F. Abbott, M.T. Grisaru and R.K. Schaeffer, Nucl. Phys. B229:372 (1983).
- [15] J.L. Gervais and A. Neveu, Nucl. Phys. B46:381 (1972);  
D.A. Kosower, Nucl. Phys. B335:23 (1990).
- [16] R. Karplus and M. Neuman, Phys. Rev. 80:380 (1950).
- [17] F. A. Berends, R. Kleiss, P. De Causmaecker, R. Gastmans and T. T. Wu, Phys. Lett. 103B:124 (1981);  
P. De Causmaecker, R. Gastmans, W. Troost and T. T. Wu, Nucl. Phys. B206:53 (1982);  
R. Kleiss and W. J. Stirling, Nucl. Phys. B262:235 (1985);  
J. F. Gunion and Z. Kunszt, Phys. Lett. 161B:333 (1985);  
R. Gastmans and T.T. Wu, *The Ubiquitous Photon: Helicity Method for QED and QCD* (Clarendon Press) (1990);  
Z. Xu, D.-H. Zhang and L. Chang, Nucl. Phys. B291:392 (1987).
- [18] G. Passarino and M. Veltman, Nucl. Phys. B160:151 (1979).
- [19] J.D. Bjorken, Stanford Ph.D. thesis (1958);  
J.D. Bjorken and S.D. Drell, *Relativistic Quantum Fields* (McGraw-Hill, 1965);  
J. Mathews, Phys. Rev. 113:381 (1959);  
S. Coleman and R. Norton, Nuovo Cimento 38:438 (1965);  
C.S. Lam and J.P. Lebrun, Nuovo Cimento 59A:397 (1969);  
C.S. Lam, Nucl. Phys. B397:143 (1993).
- [20] K. Fujikawa, Phys. Rev. D7:393 (1973);  
M. Base and N.D. Hari Dass, Ann. Phys. 94:349 (1975);

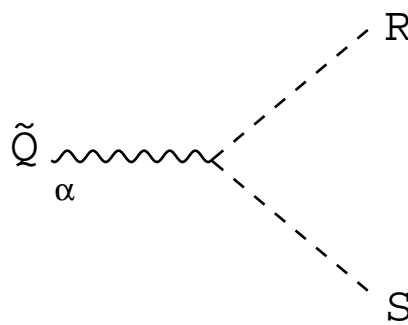
- M.B. Gavela, G. Girardi, C. Malleville and P. Sorba, Nucl. Phys. B193:257 (1981);  
 N.G. Deshpande and M. Nazerimonfared, Nucl. Phys. B213:390 (1983);  
 F. Boudjema, Phys. Lett. B187:362 (1987).
- [21] G. 't Hooft and M. Veltman, Nucl. Phys. B44:189 (1972).
  - [22] W. Siegel, Phys. Lett. 84B:193 (1979).
  - [23] G. 't Hooft and M. Veltman, Nucl. Phys. B153:365 (1979);  
 A. Denner, U. Nierste, and R. Scharf, Nucl. Phys. B367:637 (1991);  
 A. Davydychev and N.Ussyukina, Phys. Lett. B298 (1993) 363.
  - [24] Z. Kunszt, A. Signer and Z. Trocsanyi, preprint ETH-TH/93-11, hep-ph/9305239,  
 to appear in Nucl. Phys. B.
  - [25] Z. Bern, L. Dixon, and D.A. Kosower, in preparation.

## Figure Captions

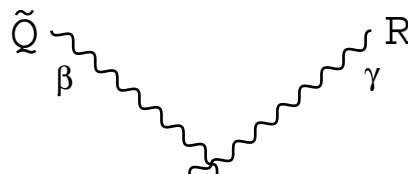
- Fig. 1:** The vertices, with coupling constants removed, needed for the calculation of boson loop contributions to  $Z \rightarrow 3\gamma$ .
- Fig. 2:** The vertices, with coupling constants removed, need for the calculation of fermion loop contributions to  $Z \rightarrow 3\gamma$ .
- Fig. 3:** The  $N = 4$  supersymmetry relations. These relations hold in the integrands of the diagrams. (For simplicity the ghost loop is implicitly included in the gauge boson loop.)
- Fig. 4:** The diagrams needed for the calculation of  $Z \rightarrow 3\gamma$ ; the loops can be either fermions, gauge bosons or scalars.
- Fig. 5:** The non-abelian three-point vertex with two gauge bosons appearing in the processes of Table 2 and the four-point vertex appearing in Table 4.



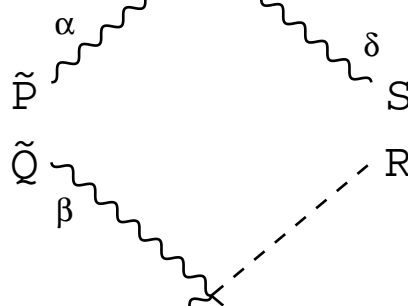
$$= i \left( g^{\beta\gamma} (k_S^\alpha - k_R^\alpha) + 2g^{\alpha\gamma} k_Q^\beta - 2g^{\alpha\beta} k_Q^\gamma \right)$$



$$= i \left( k_S^\alpha - k_R^\alpha \right)$$



$$= -2i g^{\alpha\beta} g^{\gamma\delta}$$

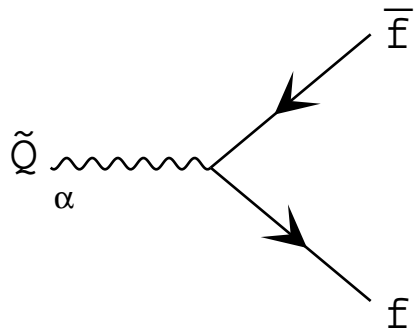


$$= 2i g^{\alpha\beta}$$

$$\begin{array}{c} k_x \rightarrow \\ \alpha \text{---} \text{---} \text{---} \beta \\ \hline -i g^{\alpha\beta} \\ k_x^2 - M_x^2 \end{array}$$

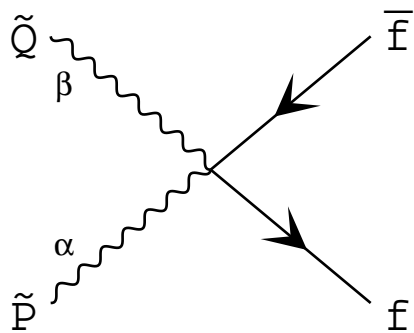
$$\begin{array}{c} k_x \rightarrow \\ \text{---} \text{---} \text{---} \\ \hline i \\ k_x^2 - M_x^2 \end{array}$$

Figure 1



$$= (k_f^\alpha - k_{\bar{f}}^\alpha) + i\sigma^{\alpha\beta} k_Q{}_\beta$$

$$\xrightarrow{k_X} \frac{-1}{k_X^2 - M_X^2}$$



$$= 2 g^{\alpha\beta}$$

Figure 2

$$6 \left( \text{Diagram 1} \right) + 4 \left( \text{Diagram 2} \right) + \left( \text{Diagram 3} \right) = \text{Simple}$$

The equation shows a sum of three Feynman diagrams, each with four external wavy lines and a central loop. Diagram 1 has a dashed loop. Diagram 2 has a solid loop with two arrows indicating a clockwise flow. Diagram 3 has a loop with a wavy internal line. Each diagram has two wavy lines on the left and two on the right, with vertical ellipses indicating continuation of the lines. The coefficients 6, 4, and 1 are placed to the left of each diagram, and the result is labeled 'Simple'.

Figure 3



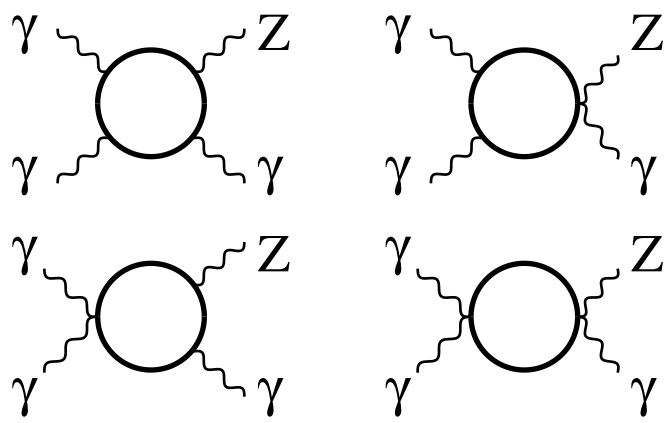
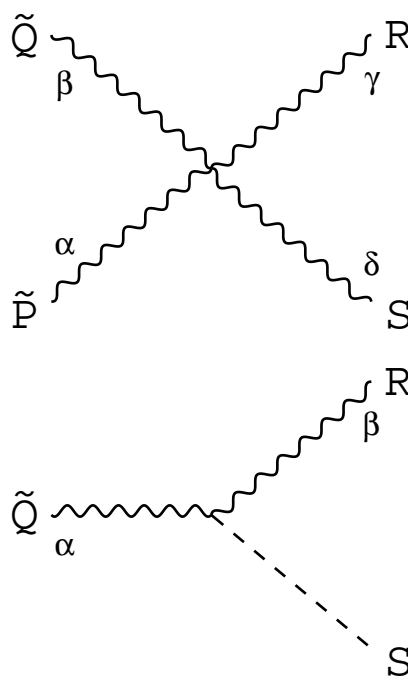


Figure 4



The figure shows two Feynman diagrams representing interactions between quarks and antiquarks via gluon and ghost exchange.

**Top Diagram (Gluon Exchange):** An incoming antiquark  $\tilde{Q}$  with index  $\beta$  and an incoming quark  $\tilde{P}$  with index  $\alpha$  interact via a gluon exchange. The outgoing particles are a quark  $R$  with index  $\gamma$  and an antiquark  $S$  with index  $\delta$ . The corresponding mathematical expression is:

$$= i \left( g^{\alpha\beta} g^{\gamma\delta} - 2g^{\alpha\gamma} g^{\beta\delta} + 2g^{\alpha\delta} g^{\beta\gamma} \right)$$

**Bottom Diagram (Ghost Exchange):** An incoming antiquark  $\tilde{Q}$  with index  $\alpha$  interacts with an outgoing quark  $R$  with index  $\beta$  via a ghost exchange. The outgoing particle is also a quark  $S$ . The corresponding mathematical expression is:

$$= i g^{\alpha\beta}$$

Figure 5